

Cite this: *RSC Sustainability*, 2025, 3, 3459

# Comprehensive assessment of phytotoxic effects, morphology, chemical compositions, and water retention capacities of biochars

Hassan El Moussaoui,<sup>a</sup> Zaina Idardare<sup>b</sup> and Laila Bouqbis<sup>\*b</sup>

The exponential increase in global organic waste production necessitates the development of efficient, economically viable, and environmentally friendly recycling methods. Pyrolysis is among the modern techniques based on the conversion of organic waste to biochars. This research focuses on evaluating the chemical compositions, water retention capabilities, phyto-toxicity, and morphology of six distinct organic biochars. Phytotoxicity assessments were conducted by subjecting lettuce and barley to varying concentrations of each biochar to evaluate chemical toxicity, while watercress was utilized to test for gaseous phytotoxic substances. Notably, no adverse effects on the germination and productivity of cress or barley were observed. However, germination and fresh lettuce weight experienced significant reduction at a 6% concentration of biochar derived from tomato waste, olive pomace biochar, municipal sewage sludge biochar and a mixture of biochar from date seeds and tomato waste. Conversely, two biochars, namely biochar from industrial agri-food sewage sludge and biochar from date seeds, exhibited no negative impact on fresh weight and lettuce germination. Furthermore, the combination between biochars decreases phytotoxic effects. Interestingly, biochar derived from tomato waste exhibited the highest water holding capacity compared to other biochars and substrates, with an average exceeding 5 g H<sub>2</sub>O per g DW. Electron microscope visualization revealed a partial inverse correlation between pore diameter and water retention. However, this relationship is not solely determined by pore size. Other critical factors, such as impurities lodged within the pores, significantly influence the water retention capacity, highlighting the complex interplay of multiple parameters in determining this property. This study emphasizes that the type of biomass and pyrolysis conditions play pivotal roles in determining the chemical, morphological, and phytotoxic properties of biochar. To harness these findings effectively it is recommended to apply these biochars at varying doses on multiple plant species.

Received 3rd January 2025  
Accepted 21st March 2025

DOI: 10.1039/d5su00005j

rsc.li/rscsus

## Sustainability spotlight

The continual rise in organic waste generation creates urgent environmental and management challenges worldwide. This research offers a sustainable solution by converting organic waste into biochar through pyrolysis, in line with the UN's Sustainable Development Goals. By analyzing water retention, chemical composition, and phytotoxic potential across different biochars, the study demonstrates how feedstock type and pyrolysis conditions influence plant growth outcomes. The findings highlight biochars that improve soil moisture while minimizing phytotoxic effects, making them more suitable for agricultural use. By turning waste into a valuable soil amendment, this work supports a circular economy, reduces landfill dependency, and enables data-driven, safe biochar application strategies.

## 1 Introduction

The challenge of meeting increasing global food needs has led to intensified agricultural practices, resulting in the degradation of water resources and soil due to poor management and excessive groundwater extraction.<sup>1-4</sup> Additionally, the

substantial volumes of waste generated from agricultural and industrial production necessitate the development of efficient and environmentally friendly waste recycling methods that are easy to implement, reduce waste volume, and benefit soil health and the environment.<sup>5</sup> Biochar, as revealed by recent studies, satisfies many of these requirements.<sup>6</sup> Produced through large-scale pyrolysis processes, biochar offers an energy-efficient approach to waste management while reducing waste size and quantity. Moreover, biochar demonstrates the ability to enhance water retention in substrates compared to control conditions, primarily attributed to its porous structure.<sup>7-10</sup> In

<sup>a</sup>Team of Biotechnology, Materials and Environment, Faculty of Sciences, Ibn Zohr University, Agadir, Morocco. E-mail: hassan.elmoussaoui@edu.uiz.ac.ma

<sup>b</sup>Ecosystems and Environmental Sciences, Faculty of Applied Sciences, Ibn Zohr University, Agadir, Morocco. E-mail: l.bouqbis@uiz.ac.ma



addition to its water retention benefits, biochar offers numerous other advantages. Appropriate biochar application rates can help reduce greenhouse gas emissions and improve the storage of organic carbon and nitrogen in the soil.<sup>11,12</sup> Furthermore, biochar application promotes microbial activity and increases crop yields,<sup>13</sup> while enhancing soil fertility and nutrient absorption in polluted soils.<sup>14</sup> However, it is important to acknowledge that some biochars may contain phytotoxic compounds, such as heavy metals, volatile organic compounds, and polycyclic aromatic hydrocarbons, which can negatively affect plant growth and the environment.<sup>15</sup> These compounds can be formed during the pyrolysis process and subsequently absorbed by the biochar.<sup>16</sup> Extracts obtained from biochars produced at high conversion temperatures have been shown to significantly suppress plant shoot growth due to the presence of phytotoxic polycyclic aromatic hydrocarbons.<sup>17</sup> Furthermore, untreated corncob biochar has been found to pose significant environmental and soil risks.<sup>18</sup> Salinity of biochar can negatively impact seedling growth and seed germination through osmotic stress, with electrical conductivity serving as an indicator of salinity levels.<sup>19–21</sup> Certain plant species, such as lettuce and tomato, appear to be more vulnerable to plant-toxic compounds present in biochar.<sup>22</sup> Additionally, the alkaline properties of biochar can affect nutrient solubility and potentially hinder plant nutrient uptake.<sup>20</sup> Numerous studies have extensively explored the phytotoxic effects of biochar, investigating its physicochemical compositions and morphological structure using diverse experimental protocols. However, there remains a significant research limitation as only a limited number of studies have examined these parameters using simplified protocols on multiple biochars simultaneously and under identical conditions. Consequently, the primary objective of this study is to address this research gap by exploring the recycling potential of a substantial quantity of waste generated in Morocco and which are widely produced throughout the world through pyrolysis using a simple reactor constructed from basic materials, eliminating the need for expensive pyrolysis equipment. Specifically, we aim to evaluate the phytotoxic effects of different biochars and mixtures to facilitate the effective recycling of large volumes of organic waste. Furthermore, our study seeks to investigate the influence of pyrolysis conditions, especially the type of feedstock, on the chemical compositions, microscopic pore size, and structure of each biochar. Additionally, we will examine how pore size affects the water retention capacity of each biochar and assess the water retention abilities of diverse biochars with three substrates sand, soil L (sandy loam), and soil A (fine silty). By accomplishing these objectives, our research aims to enhance knowledge and encourage the advantageous utilization of biochar in organic waste recycling, while also exploring its potential benefits in water and soil management practices.

## 2 Materials and methods

### 2.1 Pyrolysis reactor and operating conditions

The biochar in this study was produced using a basic pyrolysis stove fabricated in Morocco, following a model developed by

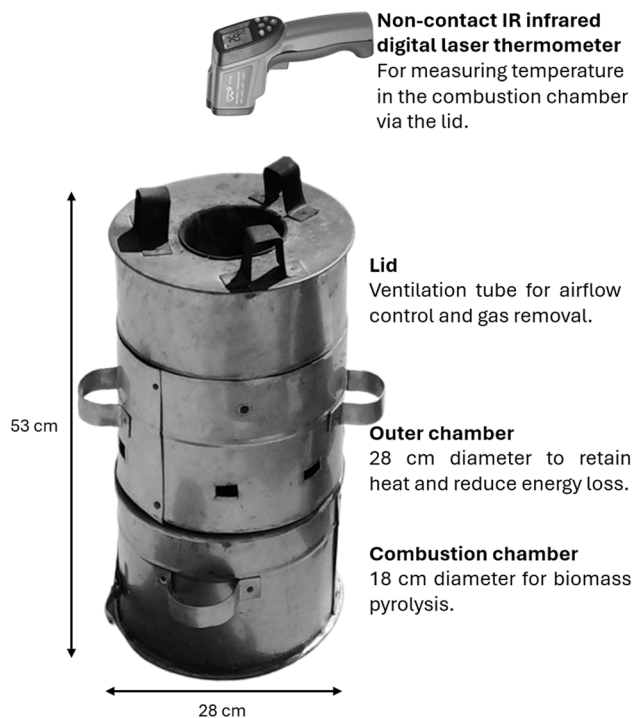


Fig. 1 Schematic image of the pyrolysis stove used for biochar production.

Prof. Dr Claudia Kammann (Department of Applied Ecology, Hochschule Geisenheim University, Geisenheim, Germany). The reactor, constructed from stainless steel for durability and efficiency, features a cylindrical structure with a height of 53 cm. It consists of an 18 cm diameter combustion chamber for biomass pyrolysis, an outer chamber with a 28 cm diameter designed to enhance heat retention and minimize energy loss, and a lid integrated with a ventilation tube to regulate airflow and facilitate the removal of gases generated during the process. The reactor's construction inherently restricts oxygen entry, creating an environment conducive to pyrolysis. While the simple design results in minor temperature fluctuations, it remains effective for achieving consistent carbonization. This accessible and low-cost system is particularly suited for promoting biochar production, encouraging practices that support carbon sequestration, organic waste recycling, and soil fertilization (Fig. 1).

### 2.2 Feedstock collection and biochar preparation

Feedstocks derived from agricultural and industrial organic waste were collected from various regions in Morocco, with consideration given to the quantity of waste produced in each region. The purpose was to recycle these feedstocks through the pyrolysis process. The feedstock consisted of two types of sewage sludge: the first was obtained from a municipal wastewater treatment plant 'RAM', while the second was recovered from an industrial agri-food wastewater treatment plant encompassing dairy, slaughterhouse, fodder, and agricultural waste 'COP'. Additionally, four other feedstocks were included



in this study: date seeds ('D'), olive pomace ('P'), Argan shells ('AR'), and waste resulting from the pruning and uprooting of tomatoes (Tomato waste 'T'). Once collected, these feedstocks were dried outdoors for 15 days. Subsequently, pyrolysis was performed in a 10 liters stainless steel simple oven. Temperatures were recorded at intervals ranging from 8 to 20 minutes "depending on the specific biomass" to ensure at least three separate measurements for each feedstock, using a non-contact IR infrared digital laser thermometer (−50 °C to 950 °C, model 'Wintact WT900', accuracy of 0.1 °C). The rate, residence time of filling and pyrolysis temperature varied for each feedstock, depending on their structural characteristics. Following pyrolysis, the resulting biochar ('BC') was crushed and sieved to a size smaller than 2 mm. Finally, the feedstock-to-biochar weight ratio was calculated to determine the productivity of each feedstock.

### 2.3. Phyto-toxic tests

**2.3.1 Cress test for gaseous phytotoxic substances.** The cress test protocol is based on the phytotoxic gas evaluation test developed and described by Busch *et al.*, (2012) and Kehres, (2006).<sup>23,24</sup> For the test, 0.5 g of cress seeds were placed on a cotton pad, which was soaked in water and positioned on an iron net over a 200 ml clear glass container. Each container was filled with two-thirds of the following substrates: "Peat" (control), BC T, BC D, BC RAM, BC P, BC COP, BC PD (a mixture of 75% BC P and 25% BC D), BC RAMAR (a mixture of 75% BC RAM and 25% BC AR), and BC TD (a mixture of 50% BC T and 50% BC D), and moistened by 30% water holding capacity. The entire experimental system was placed in a 1 liter clear glass container, kept away from light, and left undisturbed for 5 days. After 5 days, the length of 10 hypocotyls was measured, and their fresh and dry weights were determined after drying in an oven at 80 °C for 24 hours. The pH and electrical conductivity (EC) were also measured before and after the test. All tests were conducted with four replicates. A cress seedling was considered unaffected by phytotoxic gases if its fresh weight exceeded 80% of the control.

**2.3.2 Lettuce germination.** To evaluate the toxicity level and salinity impact of each type of biochar, we employed the ISO 17126 protocol titled 'Soil quality—Determination of the effects of pollutants on soil flora—Screening test for emergence of lettuce seedlings (*Lactuca sativa* L.)', as developed by Busch *et al.*, (2012).<sup>23</sup> In this test, we utilized 40 seeds of a lettuce variety (*Lactuca sativa* L.) listed in the official variety catalog of the Moroccan National Office for Food Safety (2015). Each seed batch was placed in a Petri dish containing a mixture of 100 g dry weight with 80% water holding capacity. The following biochars, including sand as the control, were tested: BC T, BC D, BC RAM, BC P, BC COP, BC PD (a mixture of 75% BC P and 25% BC D), BC RAMAR (a mixture of 75% BC RAM and 25% BC AR), and BC TD (a mixture of 50% BC T and 50% BC D). Six concentrations of biochar were applied in the test: 0.5%, 1%, 2%, 3%, 6%, and 8%. After 9 days, we recorded the number of germinated seeds and measured their fresh weight, as well as the pH and electrical conductivity (EC) before and after the test. All tests were conducted with three replicates.

**2.3.3 Barley germination and growth test.** The barley test protocol utilized in this study is based on the assessment of toxic substances, as described and developed by Busch *et al.*, (2012) and Kehres, (2006).<sup>23,24</sup> We employed 20 seeds of a specific barley variety listed in the official variety catalog of the Moroccan National Office for Food Safety since 1996. Each replicate consisted of 20 seeds placed in a 250 ml pot containing 62.5 g of the mixture to be tested, with a targeted water holding capacity of 60%. Throughout the test period, we maintained this water holding capacity by replenishing the amount of water that evaporated daily. The following biochars, with peat as the control, were tested: BC T, BC D, BC RAM, BC P, BC COP, BC PD (a mixture of 75% BC P and 25% BC D), BC RAMAR (a mixture of 75% BC RAM and 25% BC AR), and BC TD (a mixture of 50% BC T and 50% BC D). Five concentrations of biochar were applied in the test: 1%, 2.5%, 5%, 6%, and 10%. Temperature and humidity levels were monitored throughout the test period using a Datalogger UNI-T UT330B USB (temperature: −40 °C to 80 °C with an accuracy of ±0.5 °C to ±2.0 °C, humidity: 0% to 100% with an accuracy of ±3.0%). After 7 days, the number of germinated seeds was recorded, and their fresh and dry weights were measured after drying in an oven at 80 °C for 24 hours. All tests were conducted with four replicates.

### 2.4 Water holding capacity (WHC)

The water retention capacity test was conducted with three repetitions for each biochar or substrate. This experience involved using a cylindrical container measuring 5.5 cm in diameter and 3.6 cm in height, which was covered at the bottom with a permeable fabric and a filter paper. The cylinder was filled with 2/3 of each mixture intended for the respective tests. These cylinders were then placed in a plastic crate filled with water, ensuring that 95% of the cylinder height was submerged. To minimize water evaporation, the entire crate was covered with aluminum foil throughout the entire 48 hours duration of the experiment. After 24 hours, the water was emptied, and the cylinders were left undisturbed for an additional 24 hours for drainage. The water holding capacity (WHC) was calculated using the following formula:

$$\text{WHC} = \frac{(\text{Weight after draining} - \text{weight before immersion in water})}{\text{Weight before immersion in water}}$$

### 2.5 Biochar, peat and sand chemicals analysis and biochar morphology

The water extracts obtained from the samples were subjected to analysis for electrical conductivity (EC) and pH using standard electrodes. The chemical composition of the biochar, sand, and peat, in terms of total magnesium (Mg), calcium (Ca), sodium (Na), and potassium (K), was determined using a flame emission spectrophotometer. The content of zinc (Zn), manganese (Mn), iron (Fe), and copper (Cu) was analyzed using an atomic absorption spectrophotometer, following the method described by Lindsay & Norvell, (1978).<sup>25</sup> Calcination was employed to



estimate the total organic matter content (TOM), while phosphorus content was detected using the Olsen protocol.<sup>26</sup> Total nitrogen (TN) and organic carbon (OC) content were measured using the Kjeldahl method and the Walkley–Black method, respectively. Colorimetric analyses were performed to quantify potassium dihydrogen phosphate [K<sub>2</sub>HPO<sub>4</sub>] and sodium nitrate [NaNO<sub>3</sub>]. The elemental analysis and morphology of each biochar were observed using scanning electron microscopy coupled with energy-dispersive X-ray spectroscopy (EDS/SEM), employing an FEI Quanta 200-ESEM operating at 20 kV.

## 2.6 Data analysis

The effects of different biochar additions on the multiple measurements were analyzed using analysis of variance (ANOVA), and *post-hoc* comparisons between treatment groups were conducted using the Tukey test. For significance testing, a *p*-value threshold of 0.05 was used. In cases where significant differences existed between treatments (*p* < 0.05), distinct superscript letters were used to denote the differences. The result was considered statistically significant if the *p*-value was less than 0.05. The correlation between the parameters was evaluated using a quadratic polynomial representation ( $f = y_0 + ax + bx^2$ ). All statistical analyses were performed using Sigma-Plot 15.0 (Germany; TE Sub Systems Inc., 2022).

# 3 Results

## 3.1 Feedstock collection and biochar preparation

Table 1 provides insights into the relationship between feedstock characteristics and biochar production parameters, showing that the pyrolysis process varies significantly depending on the type of feedstock. The temperature ranges from 443 ± 21 °C for argan shell (AR) to 577 ± 59 °C for olive pomace (P). Olive pomace shows the highest pyrolysis temperature, reflecting the influence of feedstock composition on pyrolysis conditions. Higher temperatures, such as those observed for olive pomace (577 ± 59 °C), are likely due to the feedstock's oil content, requiring more heat to break down the material. The high oil content of olive pomace requires a higher pyrolysis temperature for effective decomposition, due to the thermal stability of lipid compounds, although a higher heating value may contribute to providing the necessary heat. This contrasts with lower temperatures for municipal sewage sludge (RAM) at 483 ± 49 °C. The residence time also varies, with municipal sewage sludge (RAM) requiring the longest pyrolysis duration at 55 min kg<sup>-1</sup>, while tomato waste (T) has the shortest at

7 min kg<sup>-1</sup>, reflecting differences in feedstock structure and density. The biochar yield from tomato waste (T) is relatively low at 12%, compared to the higher yields from other feedstocks such as municipal sewage sludge (RAM) at 60%. Notably, feedstocks with higher oil content, such as olive pomace, tend to produce lower biochar yields (15%), emphasizing the role of chemical composition in pyrolysis efficiency. This analysis highlights how different feedstocks, whether with high oil content or higher density, affect both the yield and quality of the biochar produced.

## 3.2 Phyto-toxic tests

### 3.2.1 Cress test for gaseous phytotoxic substances.

All the biochars exhibited greater fresh weight and hypocotyl length compared to the control, indicating the absence of any toxic gaseous effects from the biochar (Fig. 2). However, no significant difference was found in the average dry weight between the biochar samples and the control.

In Table 5, it can be observed that the pH and electrical conductivity (EC) values decrease after the test for all treatments, except for a slight increase in the control group consisting of peat. The initial pH of peat is acidic (5.6), while the pH of all the biochar samples is strongly basic, ranging between 9 and 11. The highest level of basicity is found in the BC TD mixture, which shows a slightly higher pH compared to its individual components (BC T and BC D). This can be attributed to a synergistic effect during mixing, where interactions between the mineral compounds of the two biochars promote the release of bases, leading to a modest increase in pH. In terms of EC, there is considerable variability both in the fluctuations after the test and in the initial values of the biochar samples. The EC of the control group remains relatively stable after the test at around 0.75 mS cm<sup>-1</sup>. Among the biochar samples, the highest EC values are observed in BC T at 39 mS cm<sup>-1</sup> and BC COP at 21.3 mS cm<sup>-1</sup>, while the remaining biochars exhibit values below 10 mS cm<sup>-1</sup>.

### 3.2.2 Lettuce germination.

Table 2 provides clear evidence of the strong alkalinity observed in the treatments both before and after testing. The electrical conductivity (EC) varies depending on the application dosage and the type of biochar used. Additionally, the table demonstrates that pH does not directly impact the germination or fresh weight of the lettuce. Typically, from our cross-referencing of biochar saline phytotoxicity data and electrical conductivity data, biochar salinity reaches an obvious phytotoxic level if it exceeds 0.6 mS cm<sup>-1</sup>. Optimal germination rates and fresh weight are generally

Table 1 Pyrolysis conditions and biochar productivity

Samples	Pyrolysis reactor filling rate (kg)	Temperature <sup>7,9,10,27,28</sup> (°C)	Yield (%)	Residence time (min)
RAM (biochar of municipal sewage sludge)	0.8 kg (ref. 7)	483 ± 49 °C	60% (ref. 7)	44 min (ref. 7)
COP (biochar of agri-food sewage sludge)	1 kg	516 ± 25 °C	32%	25 min
D (biochar of seeds of date)	2 kg	548 ± 33 °C	18%	90 min
T (biochar of tomato waste)	7 kg	530 ± 41 °C	12%	49 min
P (biochar of olive pomace)	3 kg	577 ± 59 °C	15%	105 min
AR (biochar of argan shell)	2 kg (ref. 7)	443 ± 21 °C	17% (ref. 7)	60 min (ref. 7)



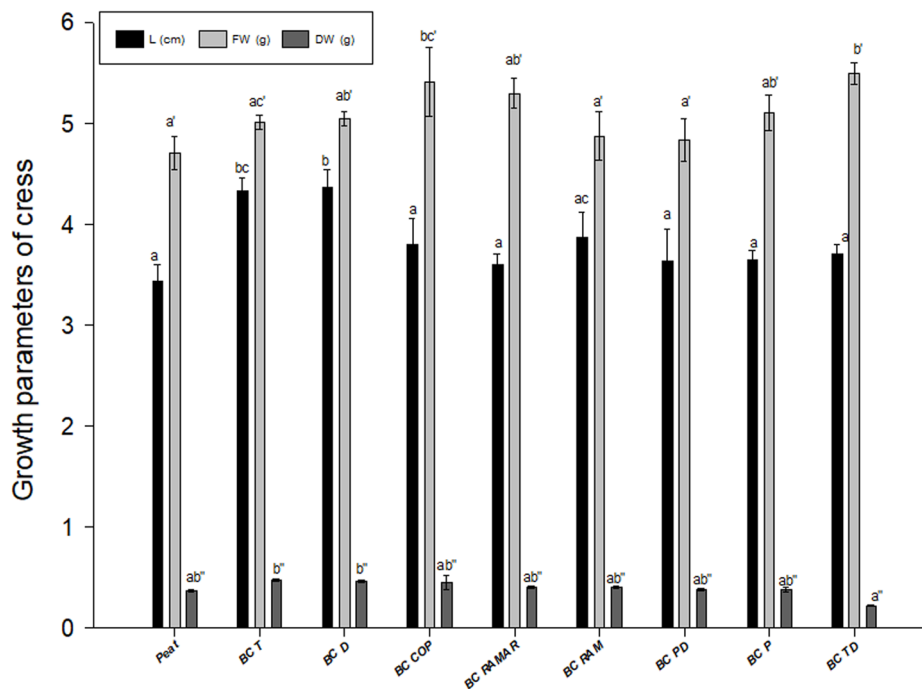


Fig. 2 Cress fresh weight (FW) in g, hypocotyl length (L) in cm, and cress dry weight (DW) in g average + standard deviation ( $n = 4$ ). Letters without ' for hypocotyl length, letters' for fresh weight, and letters'' for dry weight. BC = biochar (Feedstock source Table 1). Different letters mean significant differences between treatments at the  $p < 0.05$  level of significance. If two treatments share even a single letter, this denotes the absence of significant difference between them.

observed within an EC range of 0.1 to 0.25  $\text{mS cm}^{-1}$ . In most cases, there is a slight decrease in pH and EC after the testing period. The phytotoxic doses differ among the biochars; for BC T, even at 3% dosage, strong phytotoxicity is observed. BC RAM and BC P exhibit phytotoxic effects at 6% dosage. However, two types of biochars, BC D and BC COP, did not display any negative effects on sprouting or the fresh weight of the lettuce at any tested dosage. When biochars are mixed, a positive effect is observed in mitigating or eliminating saline phytotoxicity, as seen in the cases of BC RAMAR, BC TD, and BC PD (Table 3).

**3.2.3 Barley germination and growth test.** Table 4 reveals that none of the biochars, at any application rate, led to a decrease in barley germination, fresh weight, or dry weight. However, a noticeable reduction in barley productivity was observed in the third measurement group for all treatments, including the control, when compared to the first two measurements. This decline can primarily be attributed to the high temperature and low humidity conditions encountered during the initial days of barley germination (Fig. 3).

### 3.3 SEM images, EDX spectra and elemental composition relative of each biochar

Surface morphology of the biochars was investigated using SEM-EDX analysis. SEM micrographs were captured at various magnifications for each biochar sample (BC T ( $\times 3700$ ), BC AR ( $\times 800$ ), BC COP ( $\times 1700$ ), BC D ( $\times 1500$ ), BC P ( $\times 2300$ ), BC RAM ( $\times 3700$ )), as shown in Fig. 4 the images clearly depict the distinct structural differences among the biochars based on

their types. BC D exhibits a smooth structure with well-ordered pores, while BC T displays a rough structure with irregular pores and sharp edges. The pore characteristics, including diameter, structure, and quantity, vary both between different biochars and within the same biochar, depending on the pyrolysis conditions and feedstock nature. SEM analysis also reveals the presence of micrometer-sized pores that contribute to the biochar's microporous network. Notably, impurities are visible within the biochar pores, with variations observed between different biochars due to differences in composition, origin, and biomass nature. BC RAM and BC AR exhibit more visible impurities compared to BC T and BC COP. EDS data indicates that all biochars have a higher carbon content along with a consistent presence of oxygen. Additionally, EDS point data analysis reveals the presence of inorganic elements (such as P, Mg, Ca, Cl, K, and Na) in all biochars, although the type and quantity of these elements vary among the different biochars. BC COP displays high EDS signals corresponding to Zn, Al, and Cu elements, while several biochars exhibit signals for Cu and Fe. The SEM images and EDS spectra provide insights into the surface morphology and elemental composition of BC D, highlighting the presence of P, K, Cl, and Ca.

### 3.4 Water holding capacity (WHC)

Fig. 5 highlights the variation in water retention capacity (WHC) among different substrates and biochars. It is evident that the WHC varies depending on the type of substrate used. Generally, the substrates exhibit lower WHC compared to biochars. BC T



Table 2 pH and CE value before and after lettuce test; BC = biochar (Feedstock source Table 1)

Biochar doses	Control sand 0%						0.5% BC			1% BC			2% BC			
	Before		After		Before		After		Before		After		Before		After	
	pH	EC mS cm <sup>-1</sup>	pH	EC mS cm <sup>-1</sup>	pH	EC mS cm <sup>-1</sup>	pH	EC mS cm <sup>-1</sup>	pH	EC mS cm <sup>-1</sup>	pH	EC mS cm <sup>-1</sup>	pH	EC mS cm <sup>-1</sup>	pH	EC mS cm <sup>-1</sup>
BC T	9.08	0.1605	8.98	0.1487	9.62	0.17	9.51	0.1411	9.65	0.24	9.5	0.223	10.01	0.65	9.97	0.41
BC D	9.08	0.1605	8.98	0.1487	9.11	0.06	9.1	0.0523	9.23	0.06	9.16	0.0562	9.27	0.08	9.25	0.064
BC COP	9.06	0.16	8.9	0.1566	8.59	0.04	9.18	0.1189	9.24	0.05	9.36	0.1508	9.57	0.09	9.39	0.1727
BC RAMAR	9.06	0.16	8.9	0.1566	9.30	0.07	9.09	0.1345	9.39	0.18	8.9	0.1593	9.43	0.20	8.86	0.258
BC RAM	9.06	0.16	8.9	0.1566	9.08	0.06	8.97	0.202	9.01	0.08	8.94	0.204	9.38	0.11	8.78	0.306
BC PD	9.07	0.1612	8.88	0.1501	9.92	0.18	9.14	0.12	10.30	0.39	9.47	0.294	10.36	0.70	9.48	0.386
BC P	9.07	0.1612	8.88	0.1501	9.05	0.07	9.39	0.0498	9.22	0.09	9.25	0.056	9.25	0.11	9.38	0.1005
BC TD	9.07	0.1612	8.88	0.1501	9.37	0.12	9.31	0.0967	9.44	0.15	9.33	0.1396	9.64	0.36	9.61	0.237
Biochar doses	3% BC			6% BC			8% BC									
	Before		After		Before		After		Before		After		Before		After	
	pH	EC mS cm <sup>-1</sup>	pH	EC mS cm <sup>-1</sup>	pH	EC mS cm <sup>-1</sup>	pH	EC mS cm <sup>-1</sup>	pH	EC mS cm <sup>-1</sup>	pH	EC mS cm <sup>-1</sup>	pH	EC mS cm <sup>-1</sup>	pH	EC mS cm <sup>-1</sup>
BC T	10.07	1.81	9.94	0.458	10.23	2.58	10.08	0.888	10.24	2.98	10.08	1.327	10.08	1.327	10.08	1.327
BC D	9.36	0.11	9.29	0.1041	9.38	0.13	9.33	0.1054	9.42	0.17	9.41	0.113	9.41	0.113	9.41	0.113
BC COP	9.94	0.12	9.21	0.331	10.15	0.17	9.27	0.455	10.45	0.31	9.27	0.593	9.27	0.593	9.27	0.593
BC RAMAR	9.51	0.31	8.98	0.396	9.60	0.47	8.65	0.484	9.73	0.60	8.75	0.615	8.75	0.615	8.75	0.615
BC RAM	9.45	0.38	8.78	0.532	9.54	0.47	8.66	0.717	9.68	0.64	8.41	0.88	8.41	0.88	8.41	0.88
BC PD	10.54	1.18	10.18	1.064	10.55	1.74	10.2	1.133	10.54	2.11	10.41	2.03	10.41	2.03	10.41	2.03
BC P	9.49	0.32	9.59	0.208	9.58	0.50	9.6	0.451	9.70	0.80	9.55	0.651	9.55	0.651	9.55	0.651
BC TD	9.72	0.96	9.62	0.2811	9.81	1.35	9.71	0.4967	9.83	1.57	9.75	0.72	9.75	0.72	9.75	0.72



Table 3 Lettuce fresh weight and germination' number average + standard deviation (n = 3); BC = biochar (Feedstock source Table 1)<sup>a</sup>

Biochar doses	Control sand 0%		0.5% BC		1% BC		2% BC		3% BC		6% BC		8% BC	
	Fresh weight g	Germination	Fresh weight g	Germination	Fresh weight g	Germination	Fresh weight g	Germination	Fresh weight g	Germination	Fresh weight g	Germination	Fresh weight g	Germination
BC T	1.12 ± 0.06 a	34.33 ± 3.06 f	1.56 ± 0.18 bc	33.67 ± 1.15 f	1.65 ± 0.09 c	38.67 ± 1.15 f	1.24 ± 0.12 b	38.33 ± 0.58 f	0.68 ± 0.20 d	32.33 ± 5.51 f	0.18 ± 0.08 d	11.33 ± 2.52 g	0.07 ± 0.08 d	5.67 ± 6.35 g
BC D	1.12 ± 0.06 a	34.33 ± 3.06 f	1.49 ± 0.08 b	37.33 ± 2.08 f	1.49 ± 0.17 b	35.67 ± 2.52 f	1.46 ± 0.16 b	34.33 ± 1.53 f	1.67 ± 0.04 b	39.00 ± 1.00 f	1.62 ± 0.05 b	36.67 ± 3.06 f	1.64 ± 0.16 b	37.33 ± 3.06 f
BC COP	1.32 ± 0.06 a	34.67 ± 0.58 f	1.55 ± 0.04 a	38.00 ± 0.00 g	1.38 ± 0.19 a	34.00 ± 1.00 fg	1.52 ± 0.04 a	36.00 ± 2.65 fg	1.55 ± 0.10 a	36.00 ± 1.73 fg	1.35 ± 0.09 a	39.33 ± 0.58 g	1.38 ± 0.13 a	39.33 ± 1.15 g
BC	1.32 ± 0.06 a	34.67 ± 0.58 f	1.30 ± 0.32 a	37.67 ± 2.08 f	1.33 ± 0.19 a	39.67 ± 0.58 g	1.34 ± 0.15 a	39.33 ± 0.58 g	1.33 ± 0.10 a	38.33 ± 1.53 g	1.42 ± 0.07 a	38.00 ± 1.73 f	1.33 ± 0.05 a	36.67 ± 1.15 f
RAMAR	1.32 ± 0.06 a	34.67 ± 0.58 f	1.48 ± 0.08 a	34.33 ± 2.08 f	1.23 ± 0.08 a	34.33 ± 2.08 f	1.24 ± 0.06 a	34.00 ± 4.58 f	1.03 ± 0.19 NS	35.00 ± 6.24 f	0.86 ± 0.35 NS	33.00 ± 37.67 ± 3.06 f	0.66 ± 0.25 NS	28.00 ± 7.55 f
BC PD	1.21 ± 0.06 ad	35.33 ± 0.58 f	1.33 ± 0.10 a	38.00 ± 1.00 f	1.59 ± 0.10 a	38.67 ± 1.53 f	1.55 ± 0.25 abd	37.00 ± 3.61 f	1.39 ± 0.04 ad	37.67 ± 0.58 f	1.17 ± 0.24 d	37.33 ± 3.06 f	0.67 ± 0.03 c	35.00 ± 1.73 f
BC P	1.21 ± 0.06 a	35.33 ± 0.58 f	1.53 ± 0.09 c	39.00 ± 0.00 h	1.46 ± 0.09 bc	37.33 ± 1.15 gh	1.55 ± 0.08 b	39.33 ± 1.15 g	1.16 ± 0.08 e	36.00 ± 1.00 f	0.36 ± 0.01 e	28.00 ± 5.29 NS	0.24 ± 0.12 d	20.67 ± 8.02 NS
BC TD	1.21 ± 0.06 a	35.33 ± 0.58 f	1.62 ± 0.06 b	35.00 ± 1.00 f	1.77 ± 0.02 b	37.67 ± 2.08 f	1.22 ± 0.05 a	36.00 ± 4.00 f	1.09 ± 0.09 a	35.33 ± 2.52 f	0.12 ± 0.05 c	11.67 ± 5.5 g	0.00 ± 0.00 c	0.00 ± 0.00 h

<sup>a</sup> Each biochar was tested separately from the others against the control; NS indicates no test. Different letters mean significant differences between treatments at the p < 0.05 level of significance. If two treatments share even a single letter, this denotes the absence of significant difference between them. BC = biochar (Feedstock source Table 1).



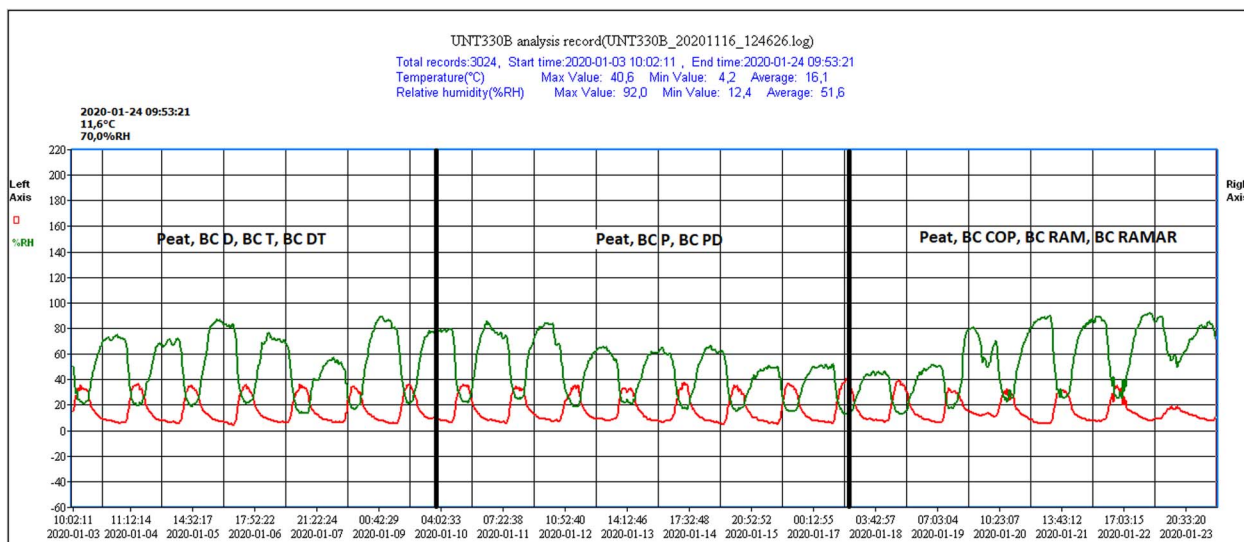


Fig. 3 Monitoring of temperature and relative humidity throughout the test period "Test of Barley": BC = biochar (Feedstock source Table 1).

and the BC TD mixture exhibit larger WHC values, measuring 5.167 and 2.633 g H<sub>2</sub>O per g DW, respectively. This enhanced water retention capacity in BC T and BC TD could be attributed to the presence of a higher number of pores with small diameters and lower levels of impurities. Additionally, it is noteworthy that the combination of biochars not only enhances germination and fresh weight of the lettuce but also increases the WHC.

### 3.5 Interaction between pore diameters and the water retention of biochar

Fig. 4 highlights the heterogeneous nature of pores in terms of diameter, structure, and number, which are strongly influenced by the pyrolysis conditions and the nature of the feedstock used. These variations directly affect the water holding capacity (WHC) across different biochars. WHC generally tends to increase with a greater number of pores and smaller pore diameters. However, the polynomial trend curve in Fig. 6, which exhibits a relatively low  $R^2$  value (0.7044), reflects significant fluctuations in the data among the different biochars. This suggests that WHC is not determined solely by pore diameter but is also influenced by additional factors such as pore homogeneity, structure, and impurities. The presence of impurities, which can partially block or alter pore functionality, and the variability in biochar properties due to differences in biomass type and pyrolysis conditions, play a crucial role in these outcomes. These factors contribute to the observed complexity in the relationship between pore size and WHC, underscoring the need to consider both physical and compositional attributes when evaluating biochar properties. This discussion contextualizes the observed fluctuations and highlights the multifaceted nature of biochar-water interactions.

### 3.6 Biochar, peat and sand chemicals analysis

Table 6 reveals significant variability in the chemical compositions of biochars, primarily attributed to differences in pyrolysis

conditions and feedstock. The total organic matter (TOM) content is notably high in BC D (92.29%) and BC AR (71.16%), reflecting their ligno-cellulosic origins. In contrast, BC P and BC RAM exhibit lower TOM values at 11.21% and 19.36%, respectively, consistent with their lower organic carbon (OC) contents of 6.50% and 11.23%. The highest OC content is observed in BC D (53.53%) and BC AR (41.28%), confirming their potential for carbon sequestration. Conversely, BC P and BC RAM display the lowest OC contents, likely due to the influence of their feedstock compositions and the basic reactor conditions that might have promoted carbon transformation into fixed carbon "the fraction of carbon remaining after volatile matter release during pyrolysis" or carbonates. BC COP and BC T show moderate TOM and OC levels at 39.69%/23.02% and 38.23%/22.18%, respectively, reflecting a balance between organic matter retention and mineral content. BC T exhibits elevated mineral content, particularly in potassium (K), sodium (Na), calcium (Ca), and magnesium (Mg). The highest phosphorus contents are observed in biochars derived from municipal and industrial sewage sludge, registering at 0.94 and 1.26, respectively. Remarkably high iron content is present in all biochars, including BC P. BC T and BC COP demonstrate the highest levels of manganese (Mn), while BC P and BC RAM exhibit the highest levels of copper (Cu). Biochars derived from various sewage sludge sources demonstrate the highest levels of zinc (Zn).

## 4 Discussion

Biochar, a carbon-rich product obtained through the pyrolysis of organic materials in a low-oxygen environment, exhibits diverse physical, chemical, and morphological characteristics influenced by the type of feedstock and production conditions.<sup>7,29</sup> The characterization of biomasses is a crucial aspect in biochar studies, as their physicochemical properties are largely influenced by both pyrolysis conditions and the composition of the biomass used. Based on data reported in the literature,



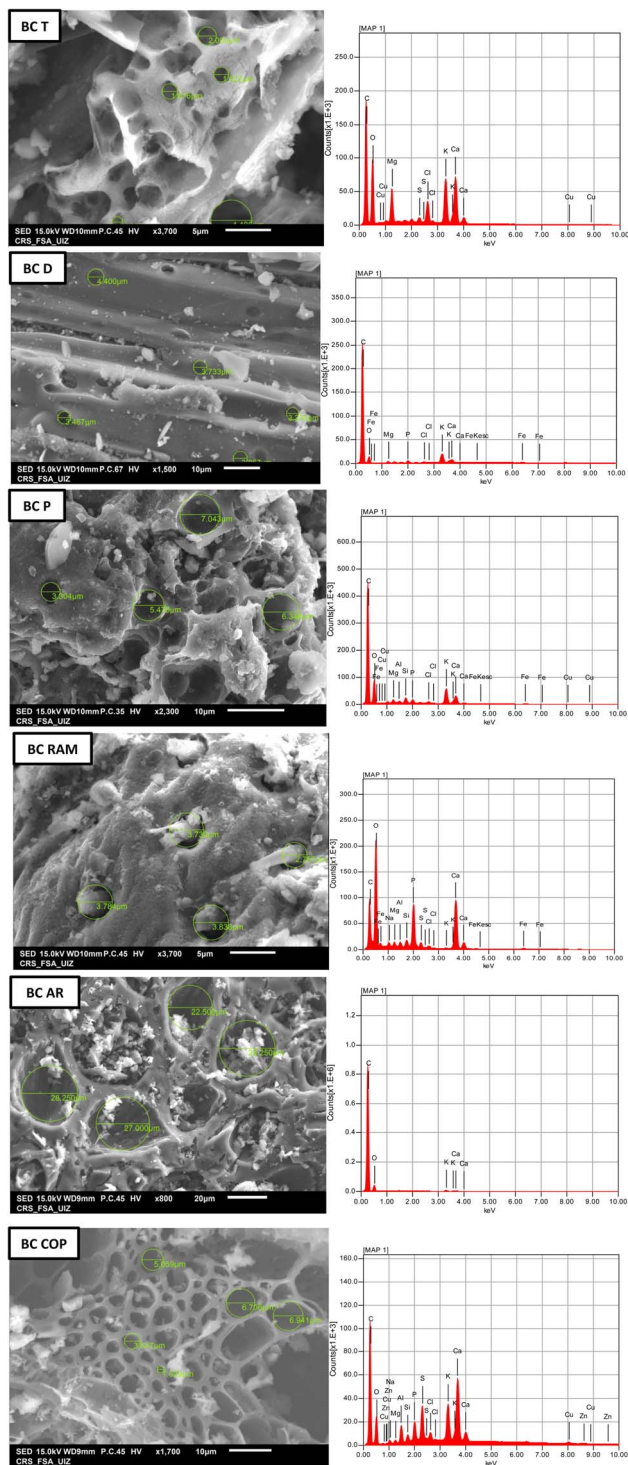


Fig. 4 SEM images and EDS spectra of surface morphology and elemental composition of each biochar.<sup>27</sup> SEM magnifications: BC T ( $\times 3700$ ), BC AR ( $\times 800$ ), BC COP ( $\times 1700$ ), BC D ( $\times 1500$ ), BC P ( $\times 2300$ ), BC RAM ( $\times 3700$ ). BC = biochar (Feedstock sources listed in Table 1).

sewage sludge typically contains carbon (C) levels of  $\sim 30$ – $50\%$ , hydrogen (H) of  $\sim 3$ – $5\%$ , nitrogen (N) of  $\sim 2$ – $6\%$ , and  $\sim 4$ – $15\%$  oxygen (O), with an ash content of  $\sim 5.6$ – $10\%$  and sulfur (S) of  $\sim 5$ – $15\%$ .<sup>30–33</sup> Similarly, date seeds have been reported to contain

$\sim 45$ – $55\%$  C,  $\sim 6.6$ – $7.5\%$  H,  $\sim 0.8$ – $0.9\%$  N, and  $\sim 44$ – $45\%$  O, with an ash content of  $\sim 7$ – $11\%$ .<sup>34</sup> For olive pomace, published studies indicate C levels of  $\sim 47$ – $55\%$ , H of  $\sim 3$ – $6\%$ , N of  $\sim 0.4$ – $2\%$ , and O of  $\sim 31$ – $38\%$ , with an ash content of  $\sim 4$ – $9\%$ , moisture levels of  $\sim 5$ – $10\%$ , and S ranging from  $\sim 0.07$ – $0.24\%$ .<sup>35,36</sup> Additionally, tomato residues have been documented to contain C levels of  $\sim 22$ – $49\%$ , H about  $7\%$ , N of  $\sim 2$ – $4\%$ , and O about  $31\%$ , with an ash content of  $\sim 9$ – $18\%$ , moisture content of  $\sim 8$ – $14\%$ , and S about  $1\%$ .<sup>37,38</sup> These reported values highlight the variability in biomass composition, which, according to the literature, directly influences biochar properties such as porosity, surface area, and nutrient content. Our study confirms that the chemical compositions and morphology of biochar are directly influenced by the starting biomass and pyrolysis conditions. Previous research has highlighted the impact of pyrolysis duration and temperature on various biochar characteristics, such as yield, surface chemistry, chemical composition, structure, and morphology. Although olive pomace has a high HHV, elevated temperatures remain necessary for efficient pyrolysis due to the structural complexity of its biomass. High-temperature pyrolysis influences biochar yield and reactivity, as demonstrated with olive husk, where increasing temperature reduces char yield but enhances gasification reactivity.<sup>39</sup> Additionally, optimizing pyrolysis requires precise temperature control, as factors such as heating rate, vapor residence time, and reactor configuration significantly impact product distribution and quality.<sup>40</sup> Furthermore, while bio-oil derived from high-energy-density biomass improves transport efficiency, the overall process still depends on thermal conditions for effective conversion as shown by Mullen *et al.*, (2010).<sup>41</sup> High temperatures lead to significant modifications in material morphology, including the loss of sintering and initial cell architecture, the formation of macro-pores, and the relative accumulation of  $\text{Ca}^{2+}$  and  $\text{Mg}^{2+}$ , as well as increased concentrations of Ca and K.<sup>42,43</sup> Our chemical analyses consistently demonstrated that BC T exhibited the highest mineral content, which can be attributed to the nutrient-rich fertigation practices used in tomato cultivation and residues from phytosanitary treatments that contribute to the accumulation of salts and minerals in tomato waste. While BC AR exhibited the lowest macroelement contents, BC RAM showed the highest heavy metal concentrations, with BC D demonstrating the lowest levels. These variations were primarily due to feedstock differences rather than pyrolysis temperature. This aligns with findings by J. W. Gaskin *et al.*, (2008),<sup>44</sup> Poultry Litter biochar compared to Peanut Hulls (PN) Pine Chips (PC) biochar had the lowest levels of analyzed macronutrients such as nitrogen (N), phosphorus (P), and potassium (K), as well as micronutrients like copper (Cu) and zinc (Zn). In terms of micronutrient content, Poultry Litter biochar showed the highest levels of metals like manganese (Mn) and iron (Fe). Moreover, as the temperature increased, some macronutrient concentrations decreased, particularly for nitrogen and potassium, with higher temperatures promoting a more stable form of biochar. However, higher pyrolysis temperatures generally resulted in increased levels of macro and microelements in biochar. Moreover, high-temperature pyrolysis enhanced water-holding



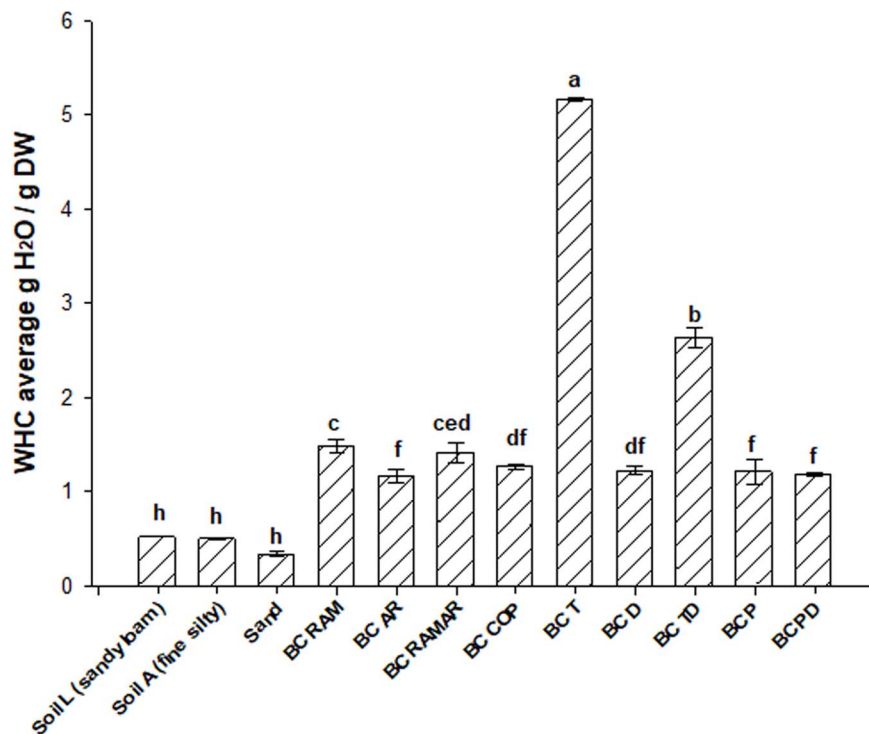


Fig. 5 WHC average g H<sub>2</sub>O per g DW average for 3 substrates and 6 biochars and 3 others biochars mixtures + standard deviation ( $n = 3$ ); different letters mean significant differences between treatments at the  $p < 0.05$  level of significance. If two treatments share even a single letter, this denotes the absence of significant difference between them. BC = biochar (Feedstock source Table 1).

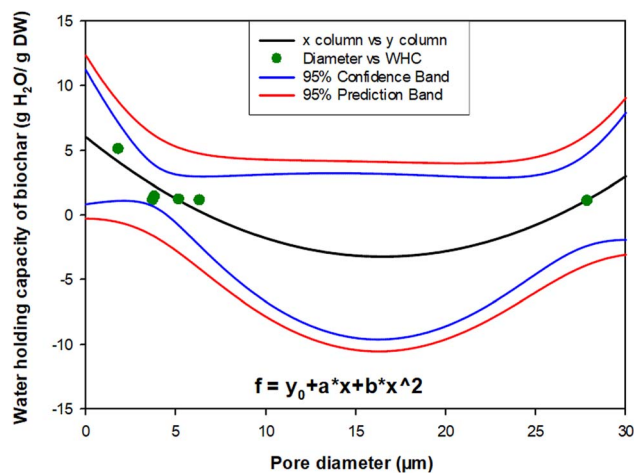


Fig. 6 Quadratic polynomial representation ( $f = y_0 + a \times x + b \times x^2$ ) of the correlation between water holding capacity (g H<sub>2</sub>O per g DW) and pore diameter ( $\mu\text{m}$ ) ( $R^2 = 0.7044$ ;  $y_0 = 6.0486$ ;  $a = -1.1220$ ;  $b = 0.0340$ ).

capacity (WHC) and the content of certain minerals, notably potassium, phosphorus, calcium, and magnesium.<sup>42,44</sup> Our results highlight the heterogeneous nature of pores in terms of diameter, structure, and number, influenced by pyrolysis conditions and feedstock type. These variations directly impact the water-holding capacity (WHC) of different biochars. Consistent with Basso *et al.*, (2013),<sup>45</sup> increasing WHC through biochar can enhance water use efficiency in sandy soils,

potentially improving agricultural productivity. Our results shows also that WHC generally increases with a higher number of pores and smaller diameters, aligning with Batista *et al.*, (2018)<sup>46</sup> who emphasized the role of surface charges and energy in water retention. However, the quadratic polynomial representation with an  $R^2$  value of 0.7044, reflects considerable fluctuations, indicating that porosity alone does not fully explain WHC variability. Factors such as impurities blocking pores and compositional variations among biochars also play a significant role, as noted by Guizani *et al.*, (2017) and J. W. Gaskin *et al.*, (2008).<sup>42,44</sup> Moreover, Adhikari *et al.*, (2022)<sup>47</sup> highlighted that optimizing biochar properties such as ageing for at least a year with enhanced oxidation, a residence time of 1 to 2 h during pyrolysis and tailoring particle size to soil texture can further improve WHC and reduce hydrophobicity. Pyrolysis of sewage sludge at high temperatures reduced yield, increased alkalinity, decreased nitrogen concentration, and elevated micronutrient levels.<sup>48</sup> Conversely, lower temperatures were associated with lower pH and electrical conductivity, higher concentrations of organic carbon, and unstable organic carbon.<sup>49</sup> Among the biochars we tested, some exhibited notably high concentrations of heavy metals that surpass the maximum limits mandated by the IBI and EBC standards for biochars intended for agricultural use.<sup>50,51</sup> Specifically, the BC COP showed a significant excess of Zn content, surpassing the maximum levels specified by the EBC. The BC T, BC P, and BC AR did not meet the required levels for Cu, while the BC RAM greatly exceeded the limits for both Cu and Zn. On the other



**Table 5** Fluctuation of pH and EC ( $\text{mS cm}^{-1}$ ) in the substrates before and after the phytotoxic test of gaseous substances; BC = biochar (Feedstock source Table 1)

	pH before test	pH after test	CE $\text{mS cm}^{-1}$ before test	CE $\text{mS cm}^{-1}$ after test
Peat	5.6	6.8	0.76	0.75
BC T	10.6	10.37	39	19.77
BC D	10.28	10.17	3.9	3.58
BC COP	10.53	9.33	21.3	3.91
BC RAMAR	9.4	8.51	3.05	2.94
BC RAM	9.39	8.36	3.93	3.36
BC PD	10.35	9.75	9.8	6.03
BC P	10.47	9.64	8.77	7.95
BC TD	11.1	10.73	33	12.15

**Table 6** Biochar, peat and sand chemicals analysis; BC = biochar (Feedstock source Table 1)

	% TOM	% OC	% N	C/N	% P	% K	% Na	% Ca	% Mg	Fe (ppm)	Mn (ppm)	Cu (ppm)	Zn (ppm)
Peat	81.83	47.46	0.74	64.15	0.07	0.47	0.08	3.25	0.64	1556.82	48.1	16.3	79.3
BC T <sup>10,27</sup>	38.23	22.18	1.21	18.29	0.36	7.70	6.14	6.83	1.56	1160.78	253.5	94.3	79.7
BC D <sup>10,27</sup>	92.29	53.53	1.64	32.61	0.23	2.21	1.06	2.49	0.41	467.62	51.2	38.3	65.2
BC P	11.21	6.50	1.60	4.01	0.33	5.94	2.51	2.50	1.49	962.74	63.0	319.4	114.6
BC RAM	19.36	11.23	0.31	36.63	0.94	0.23	2.25	10.10	1.33	7709.81	26.0	233.8	681.4
BC AR	71.16	41.28	0.29	144.48	0.36	0.68	0.36	2.84	0.32	3761.02	94.1	75.8	176.9
BC COP <sup>10,27</sup>	39.69	23.02	2.40	9.57	1.26	1.03	1.71	4.58	1.00	1590.24	129.4	28.1	283.6

	% TOM	% OC	% N	C/N	P <sub>2</sub> O <sub>5</sub> %	K <sub>2</sub> O%	Na <sub>2</sub> O%	CaO%	MgO%	Fe (ppm)	Mn (ppm)	Cu (ppm)	Zn (ppm)
Sand	1.95	1.13	0.109	10.44	0.060	0.024	0.008	4.252	1.938	1.2	4.4	0.9	3.2

hand, BC D demonstrated lower concentrations of these metals, indicating promising potential for their future development.<sup>51</sup> The results of our study on biochar show interesting similarities and differences when compared to existing literature. On one hand, our biochars exhibit significant variability in organic carbon (OC) and total organic matter (TOM) content, which aligns with the findings of Wang *et al.*, (2014),<sup>52</sup> who emphasizes the impact of pyrolysis conditions and feedstock types on biochar properties. Our BC D biochar (53.53% OC) reflects a high carbon sequestration potential, similar to biochars derived from plant materials with a high C/N ratio, as described by Gross *et al.*, (2021).<sup>53</sup> In contrast, the low OC values observed in BC P (6.50%) may be attributed to the initial composition of the biomass and temperature fluctuations in our reactor, similar to what Wang *et al.*, (2014)<sup>52</sup> reports regarding the interference of carbonates in OC analysis. Despite the beneficial effects of biochar on soil, plants, and the environment, some biochars may contain high levels of heavy metals, polycyclic aromatic hydrocarbons, or other toxic compounds.<sup>54</sup> However, specific biochars, such as those derived from peanut shell residue<sup>23</sup> or argan shells,<sup>55</sup> showed no toxic effects on germination or crop productivity. Tests on biochars produced from wheat husks and paper sludge mixture and sewage sludge with KCl additive revealed varying effects on cress and lettuce productivity, indicating potential salinity and volatile gas-related phytotoxicity.<sup>56</sup> Biochar derived from poultry litter was found to be more toxic than biochar from corn stalk, as evidenced by cress germination

tests with high ash, volatile fatty acids (VFAs), and polycyclic aromatic hydrocarbons (PAHs).<sup>21</sup> In our study, none of the tested biochars showed negative effects on cress, which can be attributed to the selected feedstock. However, most biochars tested at high doses negatively affected lettuce productivity, indicating strong contamination with toxic chemicals or salinity. Toxicity and safety assessments of biochar can be conducted using *in vitro* tests involving lung cell lines, human liver, and *in vivo* tests using *Drosophila melanogaster*. These evaluations have indicated that the toxicity of biochar is primarily determined by factors such as initial biomass, pyrolysis conditions, and biochar application concentration.<sup>57</sup> SEM images and EDX spectra analysis demonstrated the diverse shape, structure, impurity levels, and chemical compositions among different biochars, primarily influenced by pyrolysis conditions and feedstock type. Scanning electron microscopy of biochars derived from distillers' grains anaerobic digestion residue samples revealed variations in macro-porous structure, with higher temperatures during pyrolysis associated with an increased abundance of smaller-sized pores. These differences in pore size can significantly impact the chemical and physical properties of biochar, thereby influencing its potential applications.<sup>58</sup> Further research is required to fully understand the influence of pore size on biochar properties and performance. At a magnification of 1000 $\times$ , scanning electron microscopy (SEM) images highlighted the heterogeneous and porous nature of biochar surfaces, aligning with the presence of micrometer-



sized pores, which contribute to its high surface area and porous characteristics.<sup>59</sup> EDS analysis indicated that biochar exhibited higher carbon content compared to other elements. Some observed deposits were inorganic salts, likely resulting from the presence of inorganic elements detected through EDS point data analyses.<sup>60</sup> The wide range of results observed can be attributed to the biomass composition before pyrolysis.

## 5 Conclusion and perspective

Based on the results obtained in this study, it is evident that the physicochemical characteristics of biochar are directly influenced by the specific pyrolysis conditions and the type of feedstock used. The application of high doses of BC T, BC RAM, and BC P resulted in significant reductions in the fresh weight and germination rate of lettuce. However, when these biochars were combined with BC D or BC AR, the phytotoxic effects were mitigated to some extent. It is worth noting that no phytotoxic effects were observed on the productivity of barley or cress. The diameter and quality of pores have a direct impact on the water holding capacity (WHC) of biochar. Biochars with well-structured pores of smaller diameter, such as BC T, exhibited higher WHC values. To comprehensively understand the effects of temperature on the chemical and morphological parameters of biochar, further investigations are required, involving pyrolysis of the studied biomasses at different temperatures. Moreover, in order to accurately describe the effects of these biochars on soil and plants, it is essential to assess their impact on the productivity and physiological parameters of specific crops that have high water consumption, both under normal conditions and in stress conditions. Additionally, their physicochemical effects on soil and WHC should be thoroughly investigated. Given the importance of H/C org and O/C org ratios in evaluating pyrolysis efficiency and biochar stability, future studies should incorporate CHNS/O elemental analysis to complement the current characterization methods. These studies will provide valuable insights into the potential applications and limitations of biochars and contribute to the development of sustainable agricultural practices.

## Ethical statement

All authors have read, understood, and have complied as applicable with the statement on "Ethical responsibilities of Authors" as found in the Instructions for Authors.

## Data availability

Datasets generated during and/or analyzed during the current study are available from the corresponding author upon reasonable request.

## Conflicts of interest

The authors declare that they have no conflict of interest.

## Acknowledgements

The authors would like to express their sincere gratitude to the Faculty of Sciences of Agadir and the Faculty of Applied Sciences of Ait Melloul, both part of Ibn Zohr University (Agadir, Morocco), for their financial support in funding this study.

## References

- 1 A. Alam, *Int. J. Sci. Res. Agric. Sci.*, 2014, 50–55.
- 2 N. Alexandratos and J. Bruinsma, *World Agriculture towards 2030/2050: the 2012 Revision*, 2012.
- 3 H. El Moussaoui, L. F. Z. Ainlhou, A. Bourezi and L. Bouqbis, *IOP Conf. Ser. Earth Environ. Sci.*, 2022, **1090**, 012012.
- 4 R. S. Meena, *Nutrient Dynamics for Sustainable Crop Production*, 2019.
- 5 F. O. Obi, B. O. Ugwuishiwu and J. N. Nwakaire, *Niger. J. Technol.*, 2016, **35**, 957–964.
- 6 M. Tripathi, J. N. Sahu and P. Ganesan, *Renew. Sustain. Energy Rev.*, 2016, **55**, 467–481.
- 7 H. El Moussaoui and L. Bouqbis, *Sustainability*, 2022, **14**, 7270.
- 8 K. Rasa, J. Heikkinen, M. Hannula, K. Arstila, S. Kulju and J. Hyväluoma, *Biomass and Bioenergy*, 2018, **119**, 346–353.
- 9 H. El Moussaoui, Z. Idardare and L. Bouqbis, *Sci. Hortic.*, 2024, **327**, 112816.
- 10 H. El Moussaoui, Z. Idardare and L. Bouqbis, *J. Soil Sci. Plant Nutr.*, 2024, **24**, 1968–1989.
- 11 W. R. Liu, D. Zeng, L. She, W. X. Su, D. C. He, G. Y. Wu, X. R. Ma, S. Jiang, C. H. Jiang and G. G. Ying, *Sci. Total Environ.*, 2020, **734**, 139023.
- 12 G. Murtaza, Z. Ahmed, M. Usman, W. Tariq, Z. Ullah, M. Shareef, H. Iqbal, M. Waqas, A. Tariq, Y. Wu, Z. Zhang and A. Ditta, *J. Plant Nutr.*, 2021, **44**(11), 1677–1691.
- 13 H. Jia, H. Ben and F. Wu, *Processes*, 2021, **9**, 1–21.
- 14 A. Nigussie, E. Kissi, M. Misganaw and G. Ambaw, *Environ. Sci.*, 2012, **12**, 369376.
- 15 A. Freddo, C. Cai and B. J. Reid, *Environ. Pollut.*, 2012, **171**, 18–24.
- 16 S. Liao, B. Pan, H. Li, D. Zhang and B. Xing, *Environ. Sci. Technol.*, 2014, **48**, 8581–8587.
- 17 N. Rogovska, D. Laird, R. M. Cruse, S. Trabue and E. Heaton, *J. Environ. Qual.*, 2012, **41**, 1014–1022.
- 18 K. Intani, S. Latif, M. S. Islam and J. Müller, *Sustainability*, 2018, **11**, 30.
- 19 W. Buss, M. C. Graham, J. G. Shepherd and O. Mašek, *Sci. Total Environ.*, 2016, **547**, 314–322.
- 20 F. Fornes and R. M. Belda, *J. Environ. Manage.*, 2017, **191**, 237–243.
- 21 A. G. Rombolà, G. Marisi, C. Torri, D. Fabbri, A. Buscaroli, M. Ghidotti and A. Hornung, *J. Agric. Food Chem.*, 2015, **63**, 6660–6667.
- 22 G. Gascó, P. Cely, J. Paz-Ferreiro, C. Plaza and A. Méndez, *Biol. Agric. Hortic.*, 2016, **32**, 237–247.
- 23 D. Busch, C. Kammann, L. Grünhage and C. Müller, *J. Environ. Qual.*, 2012, **41**, 1023–1032.



- 24 B. Kehres, *Methodenbuch zur Analyse organischer Düngemittel, Bodenverbesserungsmittel und Substrate*, 2006.
- 25 W. L. Lindsay and W. A. Norvell, *Soil Sci. Soc. Am. J.*, 1978, **42**, 421–428.
- 26 S. R. Olsen, *Estimation of Available Phosphorus in Soils by Extraction with Sodium Bicarbonate*, US Department of Agriculture, 1954.
- 27 H. El Moussaoui, Z. Idardare and L. Bouqbis, *Water, Air, Soil Pollut.*, 2023, **234**, 606.
- 28 H. El Moussaoui, L. F. Z. Ainhout and L. Bouqbis, *Int. J. Recycl. Org. waste Agric.*, 2023, **12**, 425–440.
- 29 A. Hass and I. M. Lima, *Environ. Technol. Innov.*, 2018, **10**, 16–26.
- 30 A. Zielińska, P. Oleszczuk, B. Charmas, J. Skubiszewska-Zięba and S. Pasieczna-Patkowska, *J. Anal. Appl. Pyrolysis*, 2015, **112**, 201–213.
- 31 T. C. Sichler, D. Montag, M. Barjenbruch, T. Mauch, T. Sommerfeld, J.-H. Ehm and C. Adam, *Environ. Sci. Eur.*, 2022, **34**, 84.
- 32 S. S. Wani and M. Parveez, *Biomass Convers. Biorefinery*, 2025, 1–16.
- 33 E. Agraftoti, G. Bouras, D. Kalderis and E. Diamadopoulou, *J. Anal. Appl. Pyrolysis*, 2013, **101**, 72–78.
- 34 H. H. Sait, A. Hussain, M. Bassyouni, I. Ali, R. Kanthasamy, B. V. Ayodele and Y. Elhenawy, *Energies*, 2022, **15**, 2727.
- 35 R. Aguado, A. Escámez, F. Jurado and D. Vera, *Fuel*, 2023, **344**, 128127.
- 36 F.-M. Pellera and E. Gidakos, *J. Environ. Chem. Eng.*, 2015, **3**, 1163–1176.
- 37 J. Mokrzycki, I. Michalak and P. Rutkowski, *Environ. Sci. Pollut. Res.*, 2021, **28**, 24245–24255.
- 38 R. İlay, Y. Kavdir, M. Memici and K. Ekinici, *Int. J. Environ. Sci. Technol.*, 2020, **17**, 3917–3926.
- 39 A. Demirbas, *J. Anal. Appl. Pyrolysis*, 2004, **72**, 243–248.
- 40 A. V. Bridgwater, *J. Anal. Appl. Pyrolysis*, 1999, **51**, 3–22.
- 41 C. A. Mullen, A. A. Boateng, N. M. Goldberg, I. M. Lima, D. A. Laird and K. B. Hicks, *Biomass and bioenergy*, 2010, **34**, 67–74.
- 42 C. Guizani, M. Jeguirim, S. Valin, L. Limousy and S. Salvador, *Energies*, 2017, **10**, 796.
- 43 T. Luo, J. Zhang, M. N. Khan, J. Liu, Z. Xu and L. Hu, *Plant Sci.*, 2018, **271**, 40–51.
- 44 J. W. Gaskin, C. Steiner, K. Harris, K. C. Das and B. Bibens, *Trans. ASABE*, 2008, **51**, 2061–2069.
- 45 A. S. Basso, F. E. Miguez, D. A. Laird, R. Horton and M. Westgate, *GCB Bioenergy*, 2013, **5**, 132–143.
- 46 E. M. C. C. Batista, J. Shultz, T. T. S. Matos, M. R. Fornari, T. M. Ferreira, B. Szpoganicz, R. A. De Freitas and A. S. Mangrich, *Sci. Rep.*, 2018, **8**, 1–9.
- 47 S. Adhikari, W. Timms and M. A. P. Mahmud, *Sci. Total Environ.*, 2022, **851**, 158043.
- 48 M. K. Hossain, V. Strezov Vladimir, K. Y. Chan, A. Ziolkowski and P. F. Nelson, *J. Environ. Manage.*, 2011, **92**, 223–228.
- 49 M. I. Al-Wabel, A. Al-Omran, A. H. El-Naggar, M. Nadeem and A. R. A. Usman, *Bioresour. Technol.*, 2013, **131**, 374–379.
- 50 IBI, *Int. Biochar Initiat.*, 2015, 1–48.
- 51 European Biochar Foundation (EBC), *Eur. Biochar Found*, 2023, 1–22.
- 52 T. Wang, M. Camps-Arbestain, M. Hedley, B. P. Singh, R. Calvelo-Pereira and C. Wang, *Soil Res.*, 2014, **52**, 495–504.
- 53 A. Gross, T. Bromm and B. Glaser, *Agronomy*, 2021, **11**, 2474.
- 54 J. Ruzickova, S. Koval, H. Raclavska, M. Kucbel, B. Svedova, K. Raclavsky, D. Juchelkova and F. Scala, *J. Hazard. Mater.*, 2021, **403**, 123644.
- 55 L. Bouqbis, H. Werner Koyro, C. Kammann, L. F. Zohra Ainhout, L. Boukhalef and M. Cherif Harrouni, *E3S Web Conf.*, 2018, 02004.
- 56 L. Bouqbis, H. W. Koyro, M. C. Harrouni, S. Daoud, L. F. Z. Ainhout, C. I. Kammann and A. C. Test, *Int. J. Biol. Biomol. Agric. Food Biotechnol. Eng.*, 2016, **10**, 1–9.
- 57 X. Yang, W. Ng, B. S. E. Wong, G. H. Baeg, C. H. Wang and Y. S. Ok, *J. Hazard. Mater.*, 2019, **365**, 178–185.
- 58 X. Zheng, Z. Yang, X. Xu, M. Dai and R. Guo, *J. Chem. Technol. Biotechnol.*, 2018, **93**, 198–206.
- 59 M. Turk Sekulić, S. Pap, Z. Stojanović, N. Bošković, J. Radonić and T. Šolević Knudsen, *Sci. Total Environ.*, 2018, **613–614**, 736–750.
- 60 K. A. Spokas, J. M. Novak, C. A. Masiello, M. G. Johnson, E. C. Colosky, J. A. Ippolito and C. Trigo, *Environ. Sci. Technol. Lett.*, 2014, **1**, 326–332.

